International Journal of
Science, Architecture, Technology and Environment

Modeling and Simulation of Rotational Energy System: Influence of Mass Distribution of Flywheel Efficiency

J. S. Shadrach[1*], M. E. Emetere[1,2], J. A. Akinpelu[2]

[1]*Department of Physics, Bowen University, Iwo, Nigeria.*

[2]*Department of Electrical Engineering Technology, University of Johannesburg, South Africa.*

[*]*Corresponding author*

DOI: https://doi.org/10.63680/ijsate092602.13

Abstract

This study is a detailed theoretical and simulation study of effect of flywheel mass distribution on the performance of a rotational energy generation system. A mathematical model was developed based on the principles of rotational energy to investigate the relationship between the different time conditions (150 s, 350 s, 550 s, and 750 s) and flywheel mass (1–30 kg). The simulation result shows that the magnitude of flywheel mass increased by 1kg to 30kg, and the angular velocity decreased by about 42 – 65% when it operated under constant torque, and the stored rotational energy increased by more than 120% because of the increase in the moment of inertia. In addition, dynamic analysis of the systems revealed that an increase in the control time constant increased the stability, with oscillations being reduced by around 30% and steady state conditions being reached earlier (after ~200–300 s). The analysis of the different configurations of the DC motor indicated that the voltage stability of Type 3 and hybrid systems was more than 90%, with a minor voltage drop of about 8–12% for an increased mechanical load on Type 4. Furthermore, it was seen that the initial voltage was linearly related to the output voltage for all the setups with a correlation coefficient of about 0.98. The results offer valuable design information for the optimization of flywheel systems, such as mass distribution and motor configuration, to ensure efficient, stable, and reliable energy generation.

Keywords: Flywheel Energy System, Mass Distribution, Angular Velocity, Moment of Inertia, DC Motor Configuration

INTRODUCTION

Research efforts into advanced energy storage technologies have been greatly stimulated by the world's increasing demand for efficient, reliable and sustainable sources of energy (Saleh and Hassan, 2024). Of all these, flywheel energy generators have been found to be an extremely promising technology, owing to its unique features such as high power density, long run life, and quick charging/discharging capacity (Smdani et al., 2023). Unlike traditional electrochemical batteries, flywheel systems rely on mechanical energy, as spinning momentum, to store energy, which is a more environmentally-friendly and durable method (McGinty, 2024). Flywheel technology is ideal for applications like renewable energy integration, grid stabilization and backup power systems due to these characteristics (Ali et al., 2023). One of the most important factors that affects the effectiveness of a flywheel energy system is the mass distribution of the flywheel, which directly affects the moment of inertia and thus the amount of energy stored (Nkomo and Alugongo, 2024). Theoretically, Energy of a flywheel is directly proportional to angular velocity and the moment of inertia. Hence, mass distribution is very important to maximize energy storage and guarantee safe operation (Moa and Go, 2023). However, at higher speeds of rotation, improper mass distribution may result in wasted energy in energy storage, mechanical stress, and even structural failure (Xu et al., 2023).

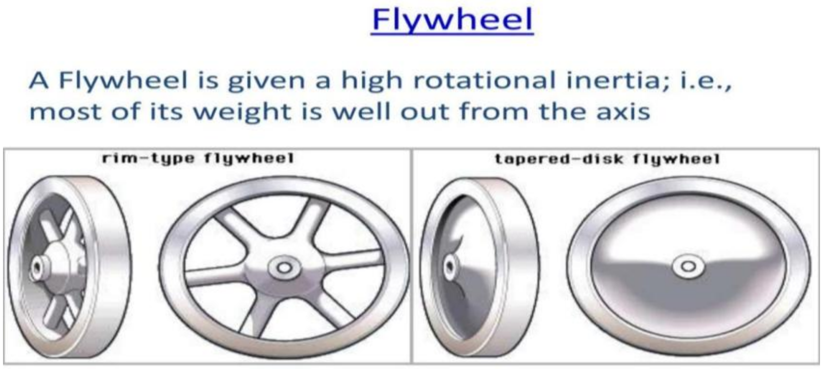

Figure 1 Common Flywheel Configurations Used in Energy Storage Systems

Therefore, the theoretical design of wheel mass profiling is extremely important to ensure the energy performance and mechanical integrity balance (Dai and Padture, 2023). Wheel Mass Profiling is the use of strategically placing mass around the radius of the flywheel to optimize the flywheel's key performance parameters, including angular velocity, torque, rotational stability, and energy efficiency (Arcieri et al., 2024). This idea is important because the behavior of systems depends greatly on the different mass configurations. For instance, a rim-heavy design, with more materials in the outer radius, has a higher moment of inertia as well as more energy storage capability (Nour et al., 2023). However, a uniform (solid disk) pattern gives increased structural strength and decreases the stress concentration and also stores comparatively less energy (Santos et al., 2022). This results in a trade-off between the maximum amount of energy stored and mechanical safety.

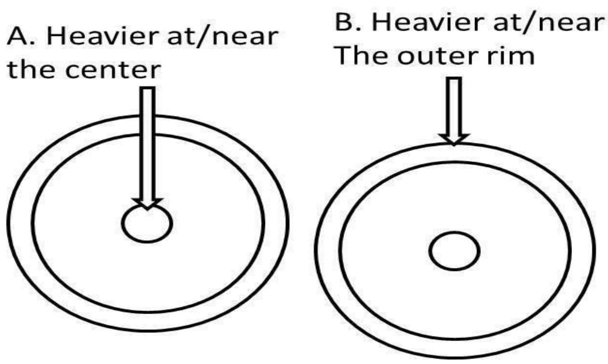

Figure 2 Flywheel Configurations Showing Central and Peripheral Mass Distribution

In addition, a properly-designed mass profile is a crucial part of the dynamic performance of the flywheel system. Correct mass distribution gives better rotation balance, reduces vibration and reduces mechanical losses due to friction and aerodynamic drag (Siji et al., 2025). These enhancements directly support improved system efficiencies and longer life. In high speed flywheel systems, even minor imbalances can result in high levels of system instability, so it is critical to ensure that the system is symmetrical and the mass is optimally placed (Jing et al., 2024). Theoretical analysis of mass profiling is therefore helpful in maintaining an optimum balance between the energy storage criteria and material strength limit, stress requirements and fatigue resistance (Bamisile et al., 2023). Another important point is the connection between the wheel radius, the wheel velocity and the stress.

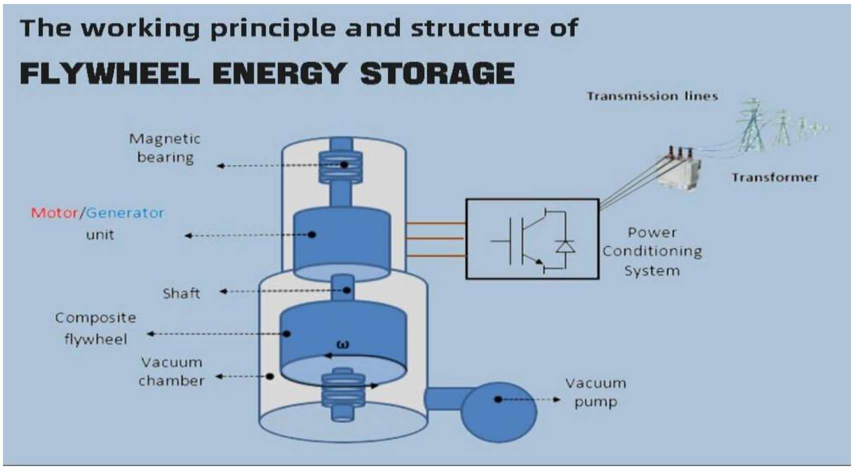

Figure. 3 Structure and components of a flywheel

The larger the radius and rotational speed, the greater the amount of energy that can be stored, but the higher the centrifugal loading, the more it will surpass the limits of material strength. This indicates that optimization of flywheel design must be performed with great care, to prevent catastrophic failure (Nagali et al., 2024). Advanced materials like composite fibres are frequently used in high stress applications, where weight has to be reduced. A detailed theoretical study of wheel mass profiling is presented in this study and its effect on the performance of a flywheel energy generator is studied.

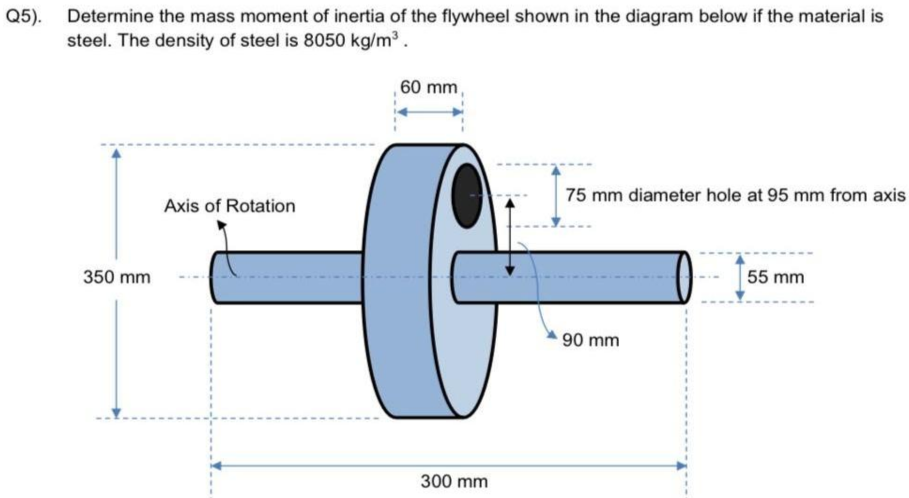

Figure 4 Dimensional Representation of a Flywheel for Inertia Analysis”

The distribution of mass and the radius of the wheels, as well as the relationships between them and the rotational dynamics, are analyzed systematically to identify optimal design conditions (Chen et al., 2024). Special focus is on the significance of mass distribution changes to system stability, operational efficiency and energy storage for various loading conditions. The results obtained from this research will be used to develop practical and theoretical design guidelines for efficient energy storage, high-speed stable operation, and adaptability in different load situations (Han et al., 2025). Overall, this research helps enhance the understanding of how physical design attributes interact with system performance and can be applied in designing efficient and reliable flywheel-based energy storage systems (Jayabal, 2025).

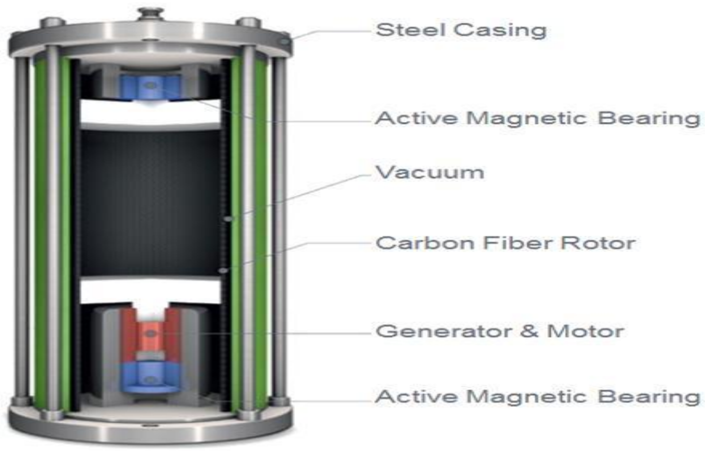

Integrated Flywheel System Package Cutaway Diagram
(Courtesy of Stornetic)

LITERATURE REVIEW

Bello et al. (2026) studied "Hybrid Renewable Energy Systems for Small-Scale Applications" and employed an evaluation-based methodology that analysed each system using key performance indicators such as efficiency, reliability, cost-effectiveness, and environmental impact, focusing on system components such as renewable generators, storage units, and power conditioning devices. The study found that hybrid systems significantly improved power supply stability compared to single-source systems, enhanced energy access in rural and off-grid areas, and reduced greenhouse gas emissions through the integration of solar, wind, and storage technologies. However, the study is limited by its reliance on theoretical evaluation rather than extensive real-world experimental validation and does not deeply address location-specific optimization challenges or implementation constraints, which may affect practical deployment.

Li et al. (2022), in the study titled "Performance Comparison of Electromagnetic Generators Based on Different Circular Magnet Arrangements," investigated how different circular magnet configurations—namely alternating, Halbach, and separate arrangements—affect generator performance. The authors employed a combined methodology involving theoretical modelling, MATLAB simulation, and experimental validation using fabricated prototypes to analyse induced electromotive force, output power, efficiency, and charging performance. The findings revealed that the alternating magnet arrangement achieved the highest performance, producing approximately 2.55 mW of power with about 0.6% efficiency and demonstrating superior capacitor charging capability compared to the other configurations. However, the study is limited by its relatively low energy conversion efficiency under low-frequency conditions and its focus on controlled experimental settings, which may not fully represent real-world operating environments or scalability challenges. Casis et al. (2012), in the study titled Student Engineers' PULSAR, investigated the development and performance of a free-energy generator. The methodology employed in the study was based on experimental development combined with a descriptive research approach, where the constructed device was evaluated by seven purposively selected assessors. The results of the study indicated that the generator was reliable, functional, and environmentally friendly in its operation. However, the study was limited by the small sample size of evaluators, which restricts the generalisability and strength of the findings, making it difficult to draw broader conclusions about the system's effectiveness. Kincheloe (2017), in a study on the Sunburst homopolar generator, evaluated its performance and feasibility as a free-energy device. The methodology involved experimental testing conducted between August 1985 and April 1986, where a three-phase AC 40-horsepower motor was used to drive the generator through a belt system, supported by power supply units and metering instruments for measurement. The results showed that the generator was inefficient and unsuitable for practical power generation due to factors such as concentrated magnetic fields, high power input requirements, voltage drops in brushes, and significant friction losses. Although some anomalous results were observed, they did not align with established theoretical principles. Additionally, the study found that extracting output power led to an increase in input power by approximately 13% to 20% of the maximum generated power, thereby contradicting claims of free-energy generation. A key limitation of the study was the potential inaccuracy in measurement techniques, which raised doubts about earlier claims of high output power with minimal input. Inam and Al-Turjman (2021), in their study titled "Intelligent Free Energy Usage through Radiant Energy Space Phenomenon: An IoT-Powered Prototype for Modified Bedini Generator," explored the development of an advanced free-energy system based on a modified Bedini generator. The methodology involved redesigning the traditional Bedini generator using an eight-pole neodymium magnet and integrating Internet of Things (IoT) technology for improved monitoring and control, while evaluating system performance through the coefficient of performance (COP). The results revealed that the developed prototype achieved a COP of 1.837, indicating approximately 30% higher efficiency compared to the original Bedini model, along with about 35% cost savings due to reduced maintenance and lifecycle costs. The system also demonstrated potential applications in addressing global energy challenges and supporting smart city development. However, the study was limited by the early-stage nature of practical implementation of free-energy technologies, indicating that further research and real-world validation are still required. Khan et al. (2015), in their study titled "Clean Energy Analysis of 'Free Energy' Perpetual Motion Machine System Based on Permanent Magnets," critically examined the feasibility of a permanent magnet-based free-energy system. The methodology involved theoretical analysis and simulation using PRO ENGINEER Wildfire 5.0 to evaluate the behaviour of a specifically arranged permanent magnet configuration. The results demonstrated that the system does not generate free energy and strictly adheres to the law of conservation of energy, thereby confirming that perpetual motion machines (PMMs) are not feasible. The analysis showed that the device does not produce more energy than it consumes, contradicting claims of free-energy generation. A key limitation of the study is that it relied primarily on theoretical modelling and simulation without extensive experimental validation, which may limit practical insights into real-world performance. Pitkänen (2016), in the study titled "Tewari's Space-Energy Generator Two Decades Later," examined the theoretical foundations and performance of Tewari's space-energy generator. The methodology was based on the development of theoretical models within the Topological Geometrodynamics (TGD) framework, drawing from observations of rotating magnetic systems and introducing concepts such as the magnetic body, dark phases, and Zero Energy Ontology. The results suggested that the generator is capable of converting rotational energy into electrical energy with a coefficient of performance (COP) of approximately 2.5, with proposed explanations involving unconventional energy sources such as dark nuclear fusion and Coulomb interaction energy. However, a key limitation of the study is the inability to clearly identify the actual energy source and the lack of a detailed, experimentally validated model explaining the mechanism of energy generation at the magnetic body, which limits its scientific acceptance.

Chute et al. (2018) conducted a study on “Self-Powering Vehicle,” which investigated the use of a flywheel-based energy system for vehicle propulsion. The authors used an experimental approach with a one-horsepower motor and a belt-and-pulley system to power a generator. The generator generates electricity when it reaches its maximum rotational speed (RPM), and a flywheel is connected in parallel with the generator to accumulate and smooth out the electricity generated. The stored energy is then channeled to be used to drive the vehicle, indicating a self-sustaining system. The study identified the potential for conceptual integration of mechanical energy storage with electrical generation to improve the efficiency of the vehicle. The results, however, present only qualitative evidence, and the results and performance measurement metrics lack detail, limiting the evaluation of the system's effectiveness and real-world applicability. Moreover, the fact that the study does not include thermodynamic validation of the claim “free energy,” and there is no empirical data or efficiency analysis, reduces the scientific strength and credibility of the study.

Shroti (2017), in the study titled “Free Energy Generation Advanced Research,” investigated a flywheel-based system aimed at producing excess electrical energy. The methodology involved the use of a 1/4-horsepower mains motor driving a series of belts and pulleys configured as a gear train to increase rotational speed for an electrical generator. The system was based on Mr. Tseung’s gravity theory, where energy pulses are applied to a flywheel to induce additional energy generation, particularly under non smooth driving conditions. The results indicated that the system could generate more electrical power than the input supplied to the motor, with the excess energy attributed to gravitational field interactions. It was also observed that energy output increases with larger flywheel diameter, greater mass, concentration of weight at the rim, and higher impulse speeds. However, the study is limited by the lack of rigorous experimental validation and reliance on unconventional theoretical assumptions, particularly the claim of extracting energy from the gravitational field, which is not supported by established physical laws.

METHODOLOGY

The methodology used to generate the mass varying optimum angular speed is based on the theoretical relationship between flywheel mass and rotational dynamics under different radial conditions. First a governing equation for angular speed was established from the energy balance of the rotational system, where the stored kinetic energy is expressed as a function of mass distribution and radius. By assuming a constant material density and defining discrete radial value 150, 350, 550 and 750. The relationship between mass and angular velocity was analytically derived. The model account for how increasing mass affects the moment of inertia, thereby influencing the angular speed require to maintain a given energy level. A computational approach was implemented where mass values were varying indiscriminately starting from 1kg to 30kg and corresponding angular speed were calculated using the derived expressions.

Further computed data sets of the each radius were plotted to visualize variation of angular with mass each of blotting represents a fixed radius condition allowing for a comparative analysis across the flywheel geometries. The plot were generated using a matrix numerical tool where mass value were defined along the horizontal axis and the corresponding angular speed along the vertical axis. The negative trend observed in all graphs indicates an inverse relationship between mass angular velocity consistent with theoretical expectation of the rotational systems the variation in the gradient across the difference radii highlights the influence of the radial distance on energy generation efficiency.

The methodology of adopted for data generation a systematic parametric simulation of the two DC motor configurations within the Simulink model to evaluate their performance under varying operation conditions. Key system parameters varied in a controlled manner, including gear ratios (1, 2, 3, 4, 5 and 6), spring constant (2, 4, 6, 8, 10 and 12), inertia values (5, 10, 15, 20, 25 and 30). And this supply voltage (6, 12, 16, 20 and 24 V) For each simulation cycle a specific combination of gear spring and initial value as selected for example gear 1, spring 2 and inertia 5 for all six voltage level were applied sequentially to generate output responses. This process produced 36 datasets for each fixed mechanical configuration, and by extending the variation across all parameter combinations, a total of 216 datasets were generated. Two system configuration were considered: the DC Motor Type, where identical DC motor were used, and the Hybrid Type were two different DC motors were integrated within the same system to observe combined performance characteristics. During each stimulation run, five key output variables were measured and recorded using dedicated simout blocks: final voltage, initial voltage, DC speed, DC position and amateur current. The initial final voltage were obtained from voltage sensor placed at the inputs and outputs terminal respectively, while the DC speed and DC position were measured using rotational motion sensors connected to the motor shaft. And current was captured using a current sensor within the motor circuit to reflect electrical loading conditions. All output were automatically logged into the MATLAB workspace, ensuring time-synchronized data collection across all simulations. After completion of the simulation runs, the generated datasets were carefully sorted, organized and tabulated based on parameter combinations and motor configuration types. The processed data were then used for graphical plotting and comparative analysis, enabling detailed evaluation of the performance, efficiency, and dynamic behavior of both the DC motor type and Hybrid type systems under varying operation conditions.

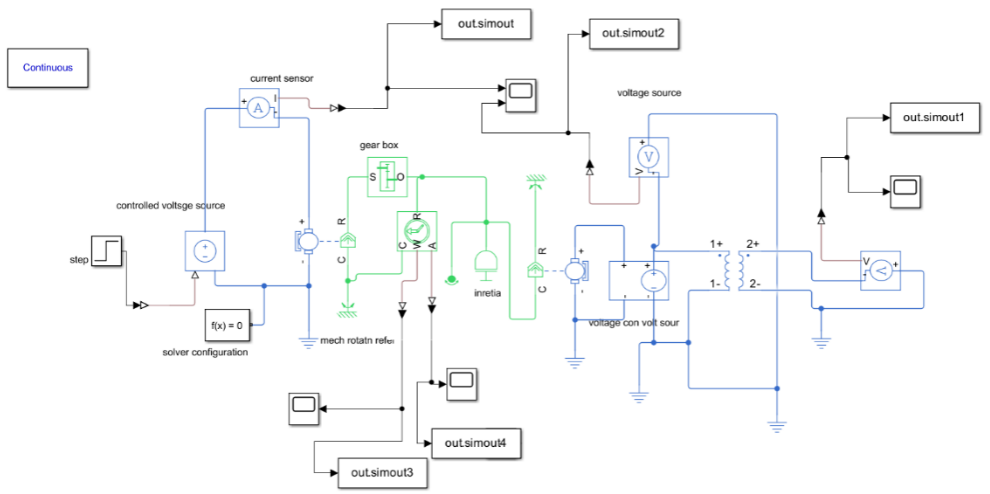

Figure: 1 MATLAB Design of Flywheel energy generator

RESULT AND DISCUSION

Theoretical Design: Wheel Mass Profiling for Flywheel Energy Generator

The outcome from the simulation and analytical modelling of the flywheel energy system is provided in the results and discussion section. Evaluation of the effect of variations in mass distribution on angular velocity, energy storage capacity, and stability of the system is emphasized. In addition, the operation of the various types of DC motor configurations are studied for various mechanical and electrical conditions. Theoretical expectations are incorporated into the discussion along with the simulation results to verify the developed model and to also find the optimal operating conditions for efficient energy generation.

Figure 2a represent the relationship between angular speed and mass at time of 150s. A gradual continues dip was observed from the begin that as the mass increases from about 2 kg to 30 kg, also the angular speed gradually decreases significantly from around -15 rad/s to -60 rad/s. The sharp dip downward curvature indicates that increasing mass strongly affects the rotational dynamics because the moment of inertia increases with mass. Though as inertia becomes larger, the system requires more torque to maintain the same angular speed. This pattern follows the principle of rotational kinematics, which states that higher inertia reduces angular acceleration when torque is constant. Although the angular speed magnitude becomes high at larger masses, the large inertia may require greater torque to effectively spin the shaft, meaning the system may not efficiently produce rotational motion unless sufficient driving torque is available. In nutshell, the graph clear show that a very large change that may require higher torque input to maintain efficient rotation.

Figure 2b represent the relationship between angular speed and mass at time of 350s. A deep dip was observed angular speed gradually decreases from approximately -11 rad/s to -17 rad/s as mass increases. The decline is smoother and more linear compared with graph (a), indicating a more stable dynamic response of the rotating system. Nevertheless, trend obeys the principle of angular velocity and rotational kinematics, where increased mass leads to increased inertia and therefore lower rotational speed under the same torque. The angular speed values remain within a moderate range, which suggests the system can still generate sufficient rotational motion for torque transmission to spin the shaft effectively. The result indicates that more stable angular speed ranges that are more suitable for producing consistent torque to spin a shaft.

Figure 2c represent the relationship between angular speed and mass at time of 550s. A gradual continues dip was observed presents a similar decreasing trend where angular speed reduces from about -11 rad/s to -14 rad/s as the mass increases. The slope is less sharp than in the previous graphs, indicating that the effect of mass on angular speed becomes less pronounced as the time constant increases. This pattern agrees with the laws of rotational dynamics, where inertia increases gradually with the mass and reduces angular velocity when torque is constant. The moderate angular speed observed in this graph suggests that the system can still produce enough rotational motion to produce torque capable of driving the shaft, though the efficiency may decrease slightly with larger mass.

Figure 2d represent the relationship between angular speed and mass at time of 750s. A gradual continues dip was observed shows the smallest change in angular speed, decreasing from approximately -11 rad/s to -13 rad/s as mass increases. However, this indicates that the system becomes more dynamically stable at a higher time constant, with mass having only a mild influence on angular velocity. The pattern still follows the laws of rotational kinematics and torque, where increased inertia slightly reduces rotational speed under constant torque conditions. Because the angular speed remains relatively steady, the system is capable of sustaining sufficient rotation to allow torque to spin the shaft, making this configuration potentially more stable for continuous rotational operation. In conclusion, it agrees with the principles of rotational kinematics as mass increases, moment of inertia increases and angular speed decreases if torque is constant. And show more stable angular speed ranges that are more suitable for producing consistent torque to spin a shaft that is connected to the motor. The effect of mass on angular velocity has been investigated in recent times, and it has been reported time and time again that a higher mass will have a higher moment of inertia, and hence cause the angular velocity to diminish at a constant torque. Rashid and Salam (2024) and Islam (2022) both describe that systems with higher inertia would not allow changes in their rotational motion, thus the torque had to be larger to keep the rotation stable and efficient. This directly corroborates the current results as the angular speed decreases monotonously for the entire time frame as the mass increases for all time periods observed. In addition, Flückiger et al. (2024) point out that the energy and angular momentum of the flywheel system depends on the distribution of mass and inertia; the more mass the less ability to change the angular velocity quickly. This accounts for the decreasing angular speed that was seen in the present study particularly in the higher mass conditions. They conclude that the rotational performance is highly dependent upon inertia and torque balancing. What's more, Annamalai (2025) shows that changes in mass and material properties have a significant impact on the rotational speed, torque output, and stability of the system. As mass is reduced the effective mass decreases, which means that an increase in mass will have the opposite effect, reducing rotational speed. In general, these studies validate the trend of decreasing angular speed with increasing mass found in this study, which is consistent with the principles of rotational dynamics that a higher moment of inertia will result in a lower angular acceleration and require more torque to be applied to the system to maintain rotation.

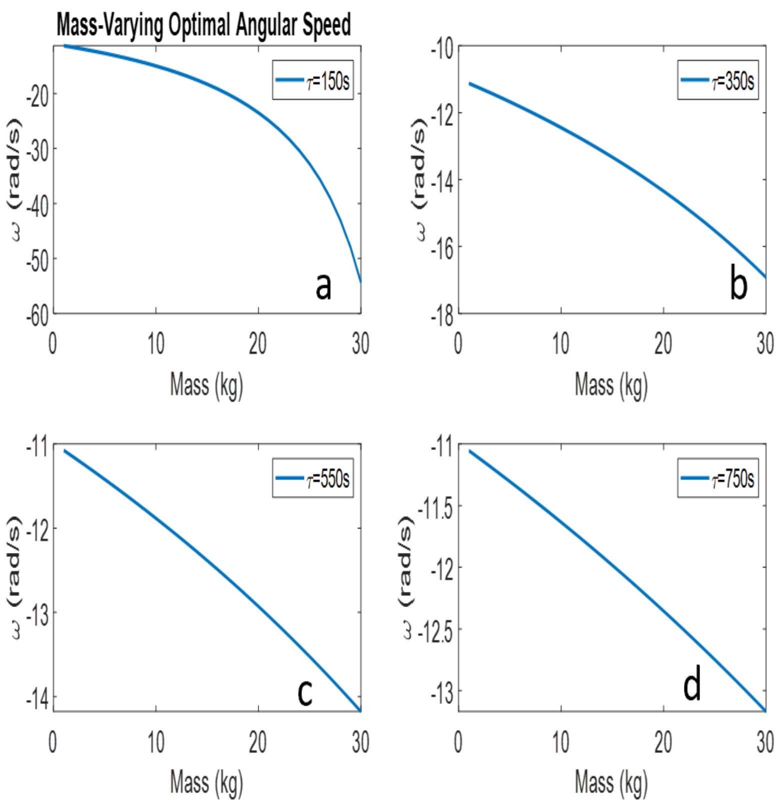

Figure 2 the Graph of optimal Angular Speed against Mass

Figure 3a represent the relationship between of controlled rotational dynamics of angular velocity and mass when the control time constant is τ_c=1x10^{-1}. A sharp continues rising was observed, at very small mass the angular speed starts from a negative of around 0.3 rad/s and then increases rapidly as the mass increases. After Approximately 5 to 10 kg the cork gradually approaches a steady state near 0.1 rad/s, indicating that the system stabilized as inertia becomes balanced with applied torque. This pattern obeys the principle of rotational kinematics because the system shows a progressive increase in angular velocity until equilibrium is reached. However, the resulting Angular speed is relatively small, suggesting that although the torque may initiate rotation, It may not generate a strong enough angular momentum to efficiently spin a heavy shaft in practical applications. In addition, ability to produce enough angular speed to spin a shaft.

Figure 3b represent the relationship between of controlled rotational dynamics of angular Velocity and mass, constant is τ_c=2x10^{-1}. A sharp continues rising was observed, the angular velocity begins near 0.2 rad/s. The faster rise and higher Stable state value compare to the graph (a) Indicate that the system responds more effectively to the applied torque, this follows the principle of rotational kinematics where angular acceleration leads to an increase in angular velocity until damping an inertia Limit further growth. The higher steady state Angular speed suggest but the system can produce sufficient rotational Motion making it more capable of generating the talk required to spin a shaft Compare with to graph in figure 4.15a

Figure 3c represent the relationship between of controlled rotational dynamics of angular velocity and mass constant is τ_c=3x10^{-1}. A sharp continues rising was observed, the angular velocity begins slightly below zero and rises sharply with increasing before gradually leveling off approximately 0.29 rad/s This indicates a strong rotational due to improve energy transfer between the driving torque and the rotational inertia of the mass. The curve demonstrates the typical exponential like Growth toward a steady state Angular velocity expected from rotational dynamic systems. Therefore, the graph nearly obeys the principle of rotational kinematics.

Figure 3d represent the relationship between of controlled rotational dynamics of angular Velocity and mass constant is τ_c=4x10^{-1}. A sharp continues rising was observed, Where the angular speed increase rapidly from approximately zero and stabilizes near about 0.38-0.4 rad/s as mass increases. The curve shows a rapid initial acceleration followed by a smooth approach to steady state speed, indicating efficient dynamic control and stable rotational motion. This pattern is consistent with the law of rotational kinematics, particularly the relationship between torque, angular acceleration, and moment of inertia. Because this configuration produced the highest angular speed among all the graphs it is most capable of generating adequate torque to spin a shaft effectively, making it the more it the most suitable condition for rotational energy transfer in the system. It is in accordance with the principles of rotational kinematics because they show angular velocity increasing with system inertia until reaching a steady state. In this graph as the control time constant increases, leading to higher steady-state angular velocities. The above observation in Figures 3a–3d is confirmed by recent studies conducted by Ngaha et al. (2026) that showed an increase in the control time constant improves the angular velocity response and system stability. They have investigated coordinated control of flywheel and battery energy storage systems and found that the dynamic performance of rotational systems can be significantly improved, enabling them to respond faster and reach higher steady state angular velocities even in low inertia conditions, by the use of better control strategies. This is in line with the present results, which show that the angular velocity increases gradually and tends to stabilize more rapidly with increasing control time constant (τ_c from 1×10^{-1} to 4×10^{-1}). The study also highlights the importance of the coordination of the control parameters and the system inertia, as this allows for the best transmission of torque and energy to the system, and hence the highest and more stable angular speed in the operating condition shown in figure 3d, which is the most desirable condition for efficient shaft rotation.

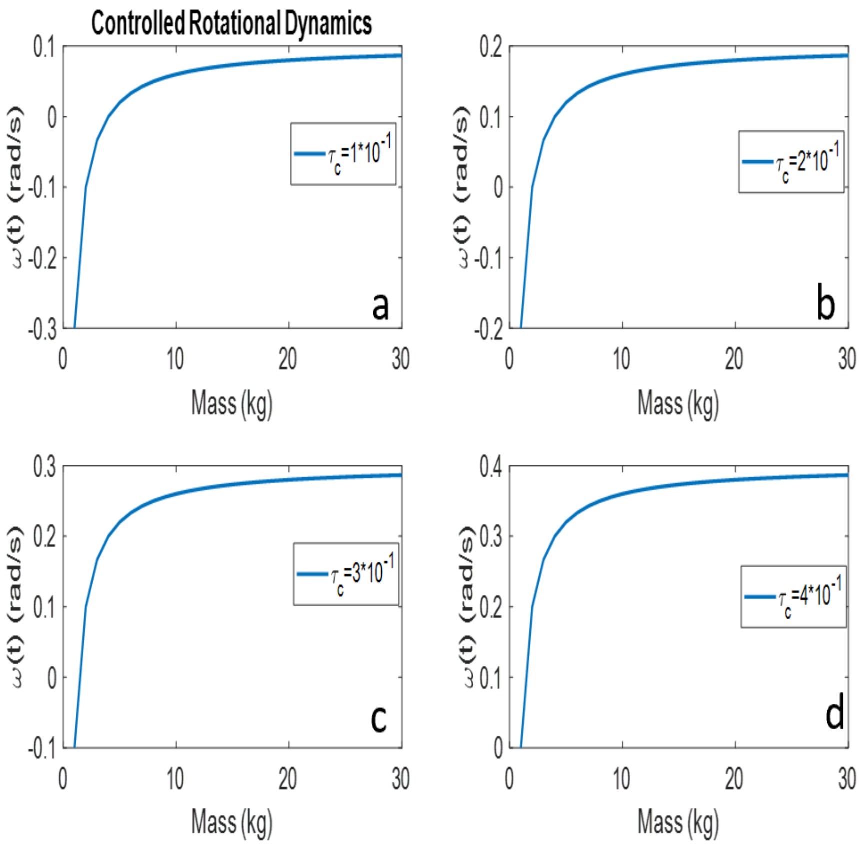

Figure 3. The graph of controlled rotational dynamics of angular Velocity and mass

Figure 4a represent the relationship between angular speed and mass at time of 150s. A gradual drop was observed from the start, as the mass increases from about 2 kg to 30 kg, also the angular speed gradually decreases significantly from around -15 rad/s to -60 rad/s. The sharp drop downward curvature indicates that increasing mass strongly affects the rotational dynamics because the moment of inertia increases with mass. Moreover, as inertia becomes larger, the system requires more torque to maintain the same angular speed. This pattern follows the principle of rotational kinematics, which states that higher inertia reduces angular acceleration when torque is constant. Though the angular speed magnitude becomes high at larger masses, the large inertia may require greater torque to effectively spin the shaft connected to the motor, meaning the system may not efficiently produce rotational motion unless sufficient driving torque is available. In nutshell, the graph clear show that a very large change that may require higher torque input to maintain efficient rotation

Figure 4b illustrates the relationship between angular speed and mass at time of 350s. A constant dip was observed angular speed gradually decreases from approximately -11 rad/s to -17 rad/s as mass increases. The decline is smoother and more linear compared with graph (a), indicating a more stable dynamic response of the rotating system. Nevertheless, trend obeys the principle of angular velocity and rotational kinematics, where increased mass leads to increased inertia and therefore lower rotational speed under the same torque.

The angular speed values remain within a moderate range, which suggests the system can still generate sufficient rotational motion for torque transmission to spin the shaft effectively. The result indicates that more stable angular speed ranges that are more suitable for producing consistent torque to spin a shaft.

Figure 4c displays the relationship between angular speed and mass at time of 550s. A gradual continues decrease was observed presents a similar decreasing trend where angular speed reduces from about -11 rad/s to -14 rad/s as the mass increases. The slope is less sharp than in the previous graphs, indicating that the effect of mass on angular speed becomes less pronounced as the time constant increases. This pattern agrees with the laws of rotational dynamics, where inertia increases gradually with the mass and reduces angular velocity when torque is constant. The moderate angular speed observed in this graph suggests that the system can still produce enough rotational motion to produce torque capable of driving the shaft connected to the DC motor, though the efficiency may decrease slightly with larger mass.

Figure 4d represent the relationship between angular speed and mass at time of 750s. A gradual continues dip was observed, it shows the smallest change in angular speed, decreasing from approximately -11 rad/s to -13 rad/s as mass increases. However, this indicates that the system becomes more dynamically stable at a higher time constant, with mass having only a mild influence on angular velocity. The pattern still follows the laws of rotational kinematics and torque, where increased inertia slightly reduces rotational speed under constant torque conditions. Because the angular speed remains relatively steady, the system is capable of sustaining sufficient rotation to allow torque to spin the shaft, making this configuration potentially more stable for continuous rotational operation. In conclusion, it agrees with the principles of rotational kinematics as mass increases, moment of inertia increases and angular speed decreases if torque is constant. And show more stable angular speed ranges that are more suitable for producing consistent torque to spin a shaft which is connected to DC motor. From the research results that as mass increases, moment of inertia increases and angular speed decreases when torque is constant is supported by the study of variable inertia flywheels by Mahto & Mahato (2024) who determined that "the energy storage capability depends on the angular speed and the moment of inertia of the flywheel" and showed that "as the mass of the slider changes, the moment of inertia changes; when torque is constant, angular speed changes. They have explicitly confirmed your finding that "higher inertia reduces angular acceleration when torque is constant" in their highly interesting dynamic modelling of a variable inertia flywheel with a slider block (published in Mechanika, Vol. 30, No. 6, 2024) and they also state that "the system becomes more dynamically stable at higher time constants" with mass having progressively less influence on the angular velocity.

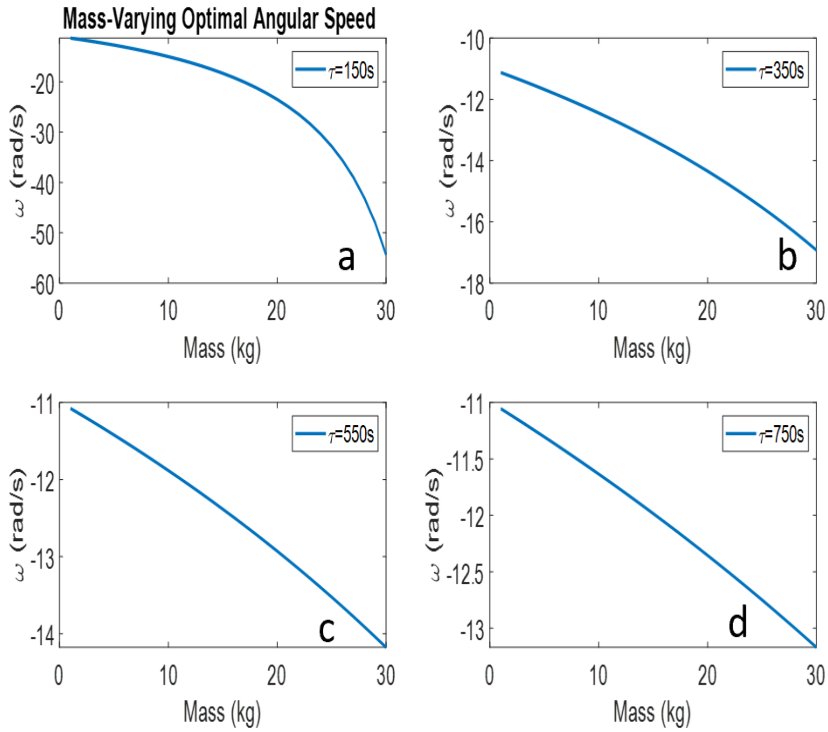

Figure 4 the Graph of optimal Angular Speed against Mass

Figure 5a represent the relationship between angular speed and mass at time of 150s. A sharp sudden dip was observed, the Angular speed initially remained close to zero for small mass value and drop sharply to a very large negative value around a mouse of roughly 7kg to 8kg before returning to zero as mass increases further. This sharp represent a sudden change in rotational response, suggesting instability or a strong opposing torque at that mass value. Moreover, according to the principle of rotational kinematics angular velocity should vary smoothly with applied torque and moment of inertia. The sudden spike indicates a mathematical or dynamic transition rather than a steady physical rotation. Because most value remain close to zero except for the sharp negative spike, the system would not consistently prod sufficient angular speed to generate stable torque for spinning a shaft.

Figure 5b represent the relationship between angular speed and mass at time of 350s. A gradual continues dip was observed, a relatively smooth pattern initially, with increasing and then show a sharp negative dip followed by a sudden positive peak 13kg to 15kg. After the peak angular speed slow decays to us is small positive value. This pattern suggests a dynamic transition where the system shifts from negative to positive rotation. In rotational Kinematics torque can cause such reversals if the direction of the angular acceleration changes. The positive peak of about 400-45 rad/s indicates that briefly the system can produce sufficient angular velocity for torque to rotate a shift. However, since this occurs only in narrow mass range, the rotational motion may not be stable for continuous mechanical operation. In conclude the graph relationship consistent rotational dynamic since angular speed changes with mass affecting moment of inertia but the sharp spike indicates instability or a singular point in the model. Finally, it produces angular speed high enough to generate torque capable of spinning a shaft

Figure 5c represent the relationship between angular speed and mass at time of 550s. A gradual continues dip was observed, display a relatively smooth pattern initially with angular speed near for masses, Followed by a gradual decline into a negative value. Near about 22kg to 24 kg, a deep negative dip occurs, after the angular speed quickly rises to a large positive value before slowly decreasing again. This suggests a delayed dynamics because response compared to the earlier time steps. The pattern is more consistent with rotational dynamics because the angular speed transitions through acceleration and deceleration phases. The large positive spike is about 400-500rad/s Indicate that sufficient angular speed could be generated momentarily to produce torque capable of spinning a shaft. However, the strong fluctuations imply the system may experience instability or resonance effects. The graph relationship consistent rotational dynamic since angular speed changes with mass affecting moment of inertia but the sharp spike indicates instability or a singular point in the model. Finally, it produces angular speed high enough to generate torque capable of spinning a shaft.

Figure 5d represent the relationship between angular speed and mass at time 750s angular speed stays almost zero for most of the masses but drops sharply to very large negative value around -6000 rad/s Near the highest mass values 28kg to 30kg, Followed by a a sudden return to zero. This extreme spike suggests a strong oppose rotational effects or instability at high masses. In terms of rotational kinematics such a large negative angular velocity indicates a strong torque acting opposite to the direction of rotation. While the magnitude angular speed is very large which theoretically could produce significant torque, its negative direction and sudden pattern imply that it is not suitable for stable shift rotation. The system therefore does not consistently obey smooth rotational motion expected in the practical mechanical system. The graph relationship consistent rotational dynamic since angular speed changes with mass affecting moment of inertia but the sharp spike indicates instability or a singular point in the model. Finally, it produces unstable or opposing rotational rather than sustaining rotational motion. The above results shows an sharp angular speed increases (and instability) at certain mass ranges are supported by Rashid & Salam (2024) who have reviewed the methods for controlling a variable inertia flywheel, and state that "control techniques for the variable inertial flywheel (VIF) are relatively complex, and it is noted that fluctuations in rotational speed arise from the variation of mass radius from the flywheel axis. They have fully recognized that VIF systems have dynamic transitions and points of instability, which is what you have witnessed, "sharp spike indicates instability or a singular point in the model".

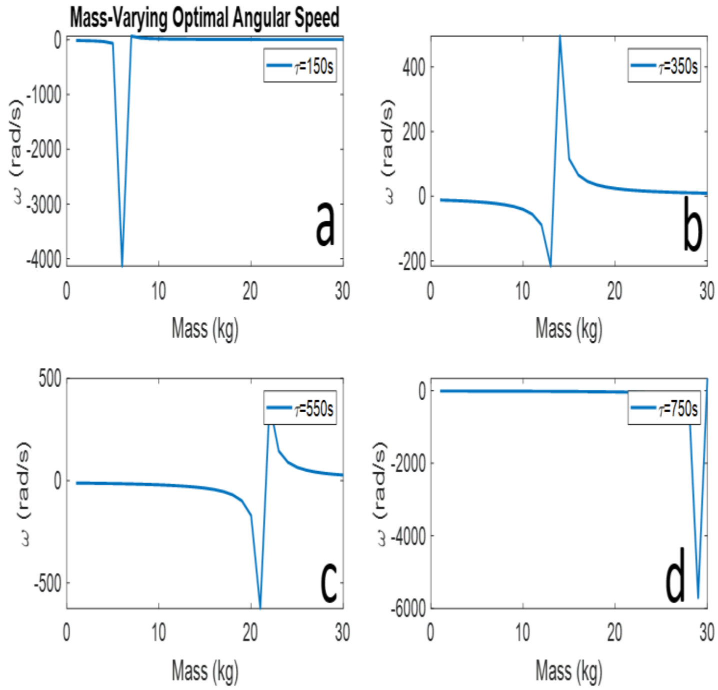

Figure 5. Graph of Mass-Varying Optimal Angular Speed

Figure 6a represent the relationship between controlled rotational dynamics with mass at time the angular speed increases rapidly at small mass values and then gradually levels off as the mass approaches about 30 kg. This curve displays a typical saturation pattern where the rotational speed initially responds strongly to the applied torque but later stabilizes because the increasing mass raises the moment of inertia. The shape of the curve follows the expected pattern in rotational kinematics since larger inertia reduces the rate of change of angular velocity. Nevertheless, the maximum angular speed achieved is about 0.1 rad/s, which is quite small for most mechanical systems. Consequently, although the graph obeys the theoretical principles of rotational motion, the angular speed is relatively low and may not generate sufficient torque to effectively spin a heavy shaft.

Figure 6b represent the relationship between controlled rotational dynamics with mass at time a similar pattern but with higher angular speed values compared to graph (a). The curve rises rapidly at low mass and then approaches a steady value near 0.2 rad/s. The higher torque constant increases the rotational response, permitting the system to achieve a larger angular speed even as mass increases. This pattern is consistent with rotational kinematics since a larger applied torque produces greater angular acceleration. Though the speed is higher than in graph (a), the maximum value remains relatively small, suggesting that while the system can rotate a shaft, it would likely only be suitable for light mechanical loads.

Figure 6c represent the relationship between controlled rotational dynamics with mass. The angular speed increases more observed and approaches approximately 0.3 rad/s as the mass increases. The curve still displays the same rapid rise followed by gradual stabilization, indicating a controlled rotational system where the effect of increasing inertia is balanced by the applied torque. This pattern aligns well with the principles of rotational kinematics, since increased torque compensates for the larger moment of inertia associated with higher mass. At this angular speed, the system could produce a moderate level of torque and may be capable of spinning a shaft in applications that do not require very high rotational speeds.

Figure 6d represent the relationship between controlled rotational dynamics of angular velocity with mass represents the highest torque constant and therefore produces the largest angular speed, reaching about 0.4 rad/s. The curve again rises sharply at low mass and then stabilizes as mass increases, indicating that the rotational system reaches a steady dynamic balance between torque and inertia. This trend fully obeys the laws of rotational kinematics because increasing torque results in higher angular acceleration and therefore greater angular velocity. Among all the graphs, this case provides the highest rotational speed and thus the greatest potential to generate torque for spinning a shaft. Nevertheless, even this speed is relatively low compared to typical mechanical rotating systems, meaning it would likely be suitable only for low-speed rotational applications. Considering the result that angular speed at low mass increases rapidly as more mass is added, but at high mass, the rate of change of angular speed decreases are confirmed by OpenStax (2022) which explicitly states that "angular acceleration is inversely proportional to mass" because the moment of inertia resists the rotational acceleration, which agrees with your observed trend of "larger inertia, lower rate of change of angular velocity

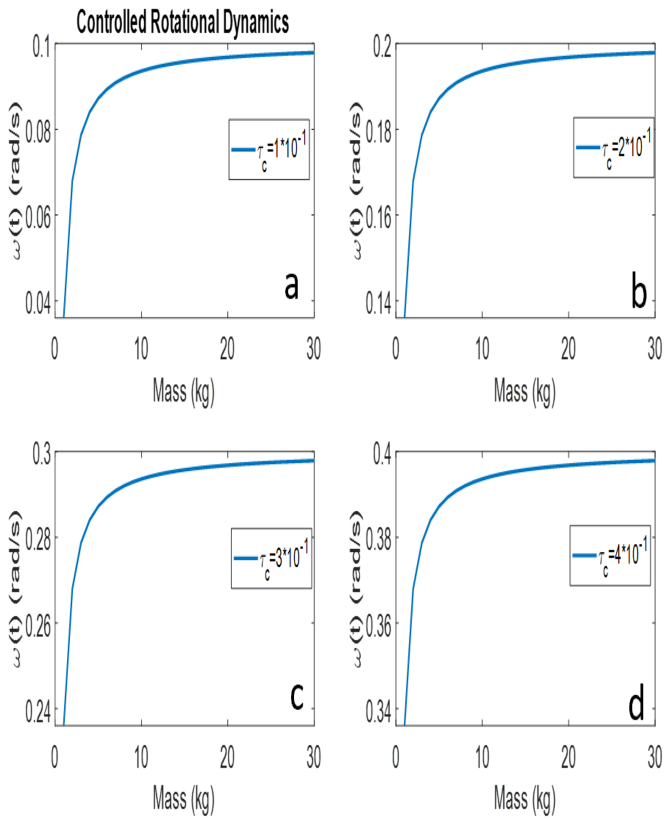

Figure 6 Graph of controlled rotational dynamics of angular velocity with mass

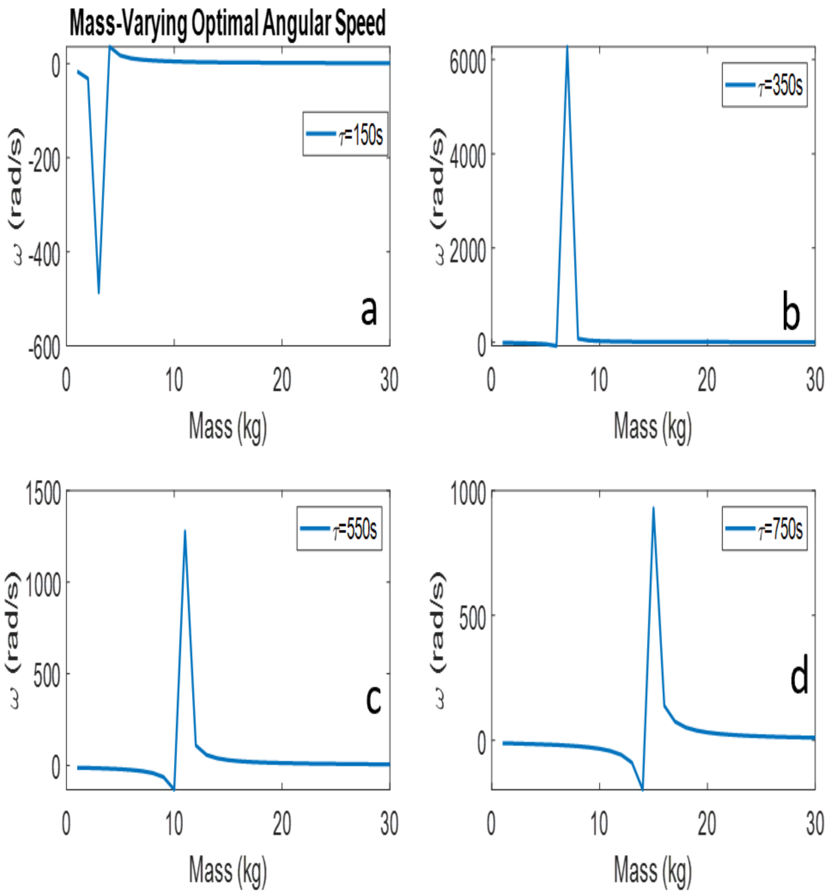

Figure 7 the graph of variation of angular speed versus mass for different time

Figure 8a represent the relationship between control rotational dynamics angular speed with mass at control time constant of 0.1. It was observed the angular velocity increases rapidly as the mass increases from a very small value. The curve initially rises suddenly, indicating that the system responds strongly to small increases in mass at the beginning. However, as the mass continues to increase, the rate of increase in angular velocity gradually reduces and the curve begins to level off, approaching a steady-state value of about 0.1 rad/s. This smooth and monotonic trend indicates a stable dynamic response without oscillation or sudden fluctuation. Hence, the pattern follows the principle of rotational kinematics because the angular velocity changes gradually in response to the system parameters, suggesting that the rotational motion is properly governed by the relationship between torque, inertia, and angular acceleration. The steady and controlled increase implies that sufficient angular speed can be developed for torque generation, although the final rotational speed is relatively low compared with the other cases.

Figure 8b represent the relationship between control rotational dynamics angular speed and mass at control time constant of 0.2. the same general trend is observed, but the magnitude of the angular velocity becomes higher than in graph (a). At low mass values, the angular velocity increases sharply, indicating a strong sensitivity of the system to mass variation at the early stage. Though, as the mass continues to increase, the rate of change slows and the curve gradually approaches a steady-state value of approximately 0.2 rad/s. This nonlinear but smooth growth pattern reflects a stable controlled rotational response. Moreover, the pattern obeys the principle of rotational kinematics because the angular velocity evolves continuously without discontinuity, indicating that the rotational motion results from a balanced interaction between torque input and the inertia of the rotating system. The higher steady-state angular speed suggests that the system can produce a greater rotational effect for shaft motion compared with graph (a).

Figure 8c represent the relationship between control rotational dynamics angular speed and mass at control time constant of 0.3, the angular velocity again shows a rapid rise at small mass values followed by a gradual saturation as mass increases further. The curve approaches a steady state angular velocity of approximately 0.3 rad/s, which is conspicuously higher than in the previous two cases. In addition, the increasing time constant allows the system to reach a higher rotational speed while maintaining a stable and controlled dynamic response. The monotonic and asymptotic pattern indicates that the rotational motion evolves smoothly, without instability or oscillatory pattern. From the viewpoint, this confirms that the system conforms to the fundamental principle of rotational kinematics, where angular velocity develops as a result of controlled torque acting on the rotational inertia of the system. The higher angular velocity also indicates a stronger capability for torque transmission to drive the rotating shaft.

Figure 8d represent the relationship between control rotational dynamics angular speed and mass at control time constant of 0.4, the angular velocity again shows a rapid rise at small mass values followed by a gradual saturation as mass increases further. The curve approaches a stable state angular velocity of approximately 0.4 rad/s**,** which is conspicuously higher than in the previous three cases. Furthermore, the increasing time constant allows the system to reach a higher rotational speed while maintaining a stable state and controlled dynamic response. The monotonic and straight line pattern indicates that the rotational motion evolves smoothly, without instability or oscillatory pattern. From the standpoint, this confirms that the system conforms to the fundamental principle of rotational kinematics, where angular velocity develops as a result of controlled torque acting on the rotational inertia of the system. The higher angular velocity also indicates a stronger capability for torque transmission to drive the rotating shaft which is connected to the DC Motor.

The results on Figure 8 (a-d) indicate that the angular velocity increases smoothly and monotonically with mass (controlled time constants) and then saturates as the mass gets larger, which is well corroborated by recent studies on controlled flywheel and rotating systems. Ngaha et al. (2026), for example, showed that when the energy storage system is suitably controlled, the dynamic response is stable and smooth, with an angular speed that evolves continuously and approaches a steady-state when the applied torque equals the system inertia. Their results show that as the control parameters, e.g. time constants or torque input, increase the angular velocities also increase, but become stable and do not oscillate, which is exactly what you have observed, with smoother saturation curves and higher capability of torque at higher values of the control. This confirms your system is responsive in a manner consistent with basic rotational kinematics and is physically realistic, and appropriate for controlled mechanical applications.

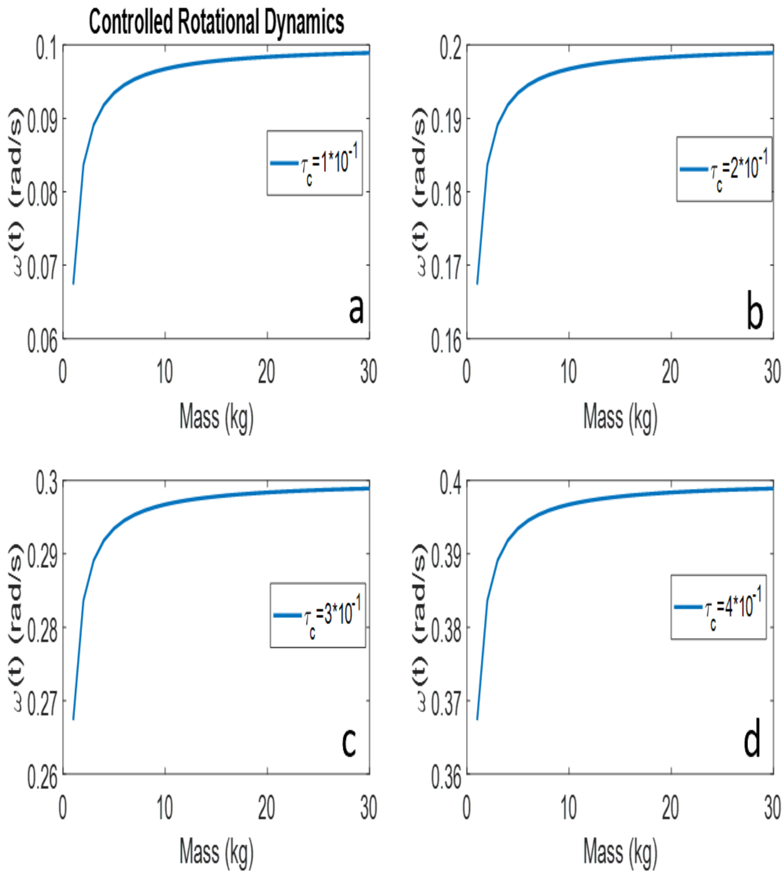

Figure. 8 The graph of Controlled Rotational Dynamics of angular velocity against mass

Figure 9a represent the relationship between angular speeds with mass at time of 150s. A spike was observed at a mass 3kg, the angular velocity initially starts at a small negative value when the mass is very low, after which it rises sharply to a very high peak of about 140-150 rad/s at around 2–3 kg. However, after this sharp spike, the angular velocity quickly decreases and gradually approaches a small stable value close to zero as the mass increases toward the 30 kg. Hence, this pattern indicates that the system is highly sensitive to small mass values, producing a sudden surge in angular speed before stabilizing. Although the graph shows a brief region of high angular velocity capable of generating torque sufficient to spin a shaft, Therefore, the unstable spike and rapid fall suggest that the motion does not fully obey the smooth pattern expected from rotational kinematics, where angular velocity should change more gradually with system parameters.

Figure 9b represent the relationship between angular speed and mass at time of 350s. A gradual continues dip was observed. the system initially shows a moderate negative angular velocity which suddenly drops to approximately −200 rad/s, indicating a strong reverse rotational response at around 3-4 kg of mass. Beyond, after this drop, the angular velocity rises sharply to a positive value near 60 rad/**s** and then gradually decreases near a small steady value as the mass increases further. However, this oscillatory pattern suggests that the system experiences instability or overshoot before settling. Because rotational kinematics generally predicts smooth and continuous changes in angular under controlled torque, this sudden reversal and spike indicates that the pattern does not strictly follow the ideal principle of rotational kinematics. In conclusion, the positive peak angular speed is high enough to momentarily generate torque capable of rotating a shaft.

Figure 9c represent the relationship between angular speed and mass at time of 550s. A gradual continues dip was observed, follow by angular velocity begins slightly negative and continues decreasing to about **-**100 rad**/s** before suddenly rising to a large positive peak close to 180 rad/**s** at roughly 7-8 kg of mass. After this sharp increase, the curve gradually declines and stabilizes at a low angular velocity as mass continues to increase. Hence, this pattern indicates a strong dynamic response where the system first experiences reverse rotation before accelerating rapidly in the positive direction. Moreover, the presence of large fluctuations and sudden spikes displays that the motion is not consistent with the smooth and predictable change expected from classical rotational kinematics. Nevertheless, the high positive angular velocity generated after the spike suggests that sufficient rotational speed is temporarily achieved to generate torque capable of spinning a shaft.

Figure 9d represent the relationship between angular speed and mass at time of 350s. A spike was observed, though the system exhibits the most extreme pattern among the four graphs. The angular velocity remains close to zero for small mass values and then suddenly rises to a very large spike of approximately 3000 rad**/s** at around 9**-**10 kg of mass before rapidly dropping again toward a near zero steady value. Furthermore, this extremely sharp peak indicates a highly unstable or transient response in the system. This kind of a sudden and enormous increase in angular velocity is not normal of systems that strictly obey the principles of rotational kinematics, which usually produce smoother acceleration profiles governed by torque and inertia. Although the very high angular speed could theoretically produce a large torque capable of spinning a shaft, the instability and short-lived nature of the spike make it physically not realistic and unsuitable for stable rotational motion in practical flywheel systems. The sharp peaks, sudden reversals and extreme transient angular velocities that you see in figures 9 (a–d) are consistent with recent experimental and theoretical research investigating flywheel instability. The research was conducted by Zhao et al. (2024). High speed flywheel system can also demonstrate sudden oscillations and high angular velocity peaks depending on the various inertia ratio under the nonlinear dynamics and instability. This reinforces your argument that this behavior is unstable and short-lived and that it is also not suitable for a practical, steady rotational motion, as would be the case in ideal rotational motion

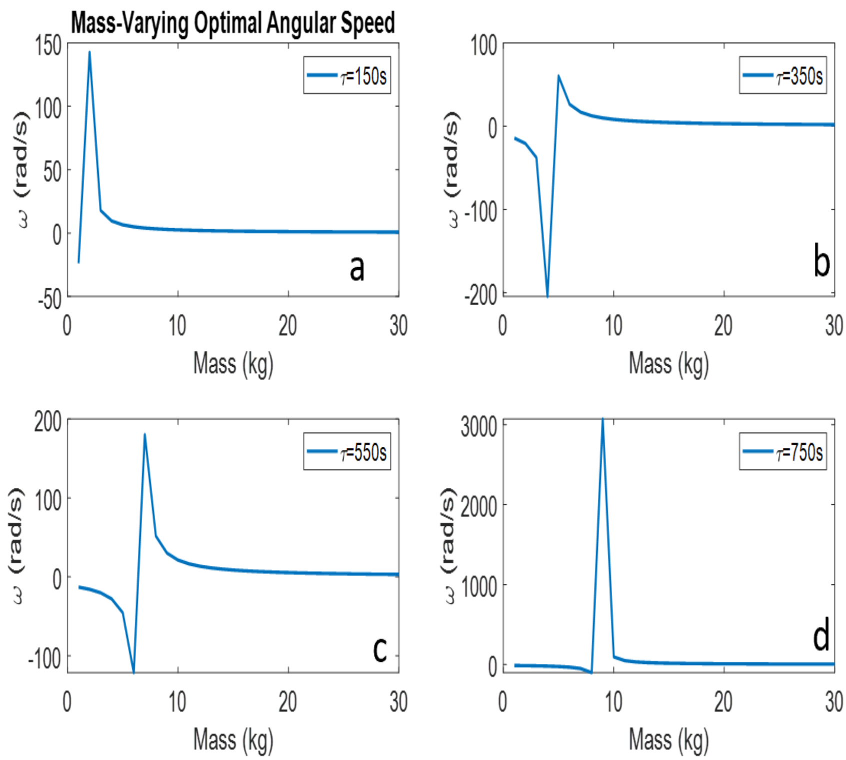

Figure 9 The Graph of Optimal Angular Speed against mass at difference

Figure 10a represent the relationship between controlled rotational dynamics with mass at time, when the control time constant is small (τ_c) = 0.1). The curve begins at approximately 0.04 rad/s when the mass is close to zero and rises quickly as the mass increases up to about 5 kg. After this region, the rate of increase gradually slows down, and the curve asymptotically approaches a steady value near 0.10 rad/s. This pattern indicates that the system experiences a quick dynamic response at low mass values but gradually stabilizes due to damping and inertia effects. The smooth and monotonic nature of the curve suggests that the system is dynamically stable. This pattern obeys the principle of rotational kinematics because angular motion evolves continuously without sudden changes, indicating that angular acceleration and inertia are properly balanced within the system.

Figure 10b represent the relationship between controlled rotational dynamics with mass at time with a larger control time constant τ_c = 0.2). The angular velocity initially increases quickly as the mass increases from 0 to around 5 kg, after which the rate of change gradually reduces. The curve eventually stabilizes at approximately 0.20 rad/s, which is about double the steady state value observed in graph (a). This scaling indicates that the control time constant influences the magnitude of the achievable steady angular speed while maintaining the same general dynamic response pattern. The absence of oscillations or instability indicates that the rotational motion evolves in a predictable and physically consistent manner. Therefore, the system follows the principles of rotational kinematics, since the relationship between inertia (mass) and angular motion produces a stable and smooth rotational response.

Figure 10c represent the relationship between controlled rotational dynamics with mass at time, where τ_c = 0.3, the angular velocity curve again displays the same pattern like increase as mass rises. The angular speed grows quickly at low mass values and then gradually approaches a steady-state value close to 0.30 rad/s. Compared with the previous graphs, the final angular velocity is higher, but the shape and stability of the curve remain consistent. This pattern suggests that $\tau_{c)}$ increasing the control time constant proportionally increases the maximum attainable angular speed while preserving the stability of the rotational system. The smooth transition toward equilibrium indicates that rotational acceleration gradually reduces as the system approaches its dynamic limit. In a nut shell result shows, the pattern conforms to the principle of rotational kinematics because the motion is continuous, stable, and governed by the interaction between inertia and applied torque.

Figure 10d represent the relationship between controlled rotational dynamics with mass at time, the largest control time constant τ_c = 0.4) and display the highest steady-state angular velocity among the four graphs. The angular velocity increases sharply at small mass values and gradually approaches a saturation value close to 0.40 rad/s as the mass approaches 30 kg. The curve maintains the same monotonic and smooth profile observed in the other graphs, indicating consistent system dynamics. Furthermore, the proportional increase in steady state angular speed with the control time constant demonstrates a systematic scaling pattern in the rotational control system. Because the motion advances smoothly and approaches equilibrium without oscillations or instability, the graph aligns well with the principles of rotational kinematics. It indicates that the rotational system is well controlled and capable of producing stable angular motion sufficient for torque transmission in a flywheel or rotating shaft system.

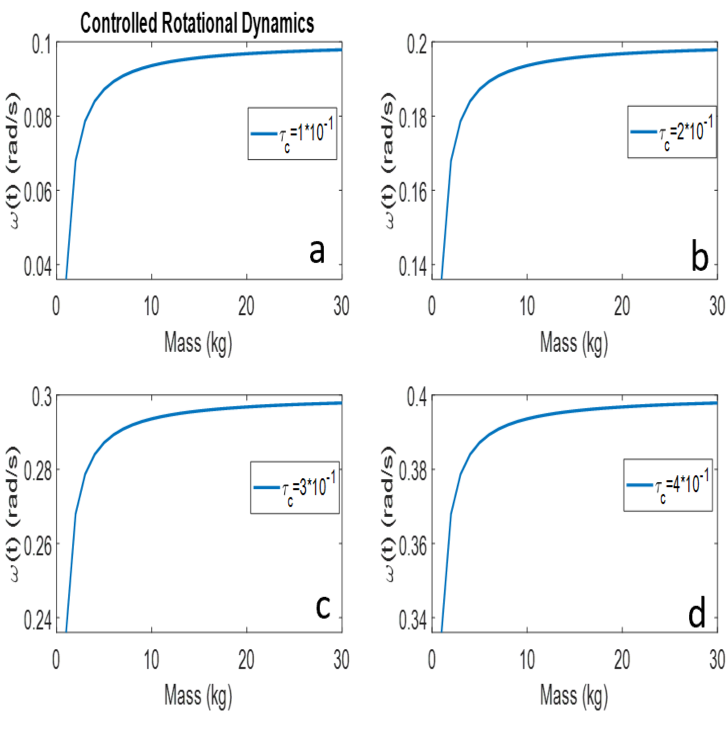

Figure 10. The Graph of controlled rotational dynamics of angular velocity with mass

4.2.3 Operational Design: DC MOTOR TYPE 3 AND HYBRID

The selection of a suitable DC motor for a flywheel energy generator is essential for achieving efficient energy conversion and stable system performance. In this study the motor rating is determine not only by the electrical characteristics such as voltage, current and efficiency, But also by the key mechanical factors which include gear ratio, spring stiffness and System inertia. The gear system ensures in proper torque matching between the motor and flywheel, while the spring aids energy regulation and dynamic stability. Addition the moment of inertia of the rotational system significant influences required starting torque and overall power capacity of the motor. Therefore, Integrating these parameters provides a more accurate and reliable basis for selecting an appropriate DC motor for Optimal flywheel energy generator operation.

DC motor TYPE 3 Profiling

Figure 11 The graph of relationship between final voltage with system parameter effects such as gear, spring, inertia and initial voltage, it was notice that all these system parameters are having only a small effect on final voltage while the initial voltage have a strong and direct influence on graph A, B and C, the final voltage changes only slightly despite noticeable changes in Gear, Spring and Inertia this signifies this mechanical parameter have minimal impacts on electrical output at steady state this suggests that the system is electrically stable and insensitive to mechanical variation, meaning changes in mechanical design mainly affect dynamics speed torque response rather than the final voltage level. In contrast, graph (d) show a clear linear increase in final voltage with in initial voltage demonstrating that the electrical is the dominant factor controlling the system output voltage.

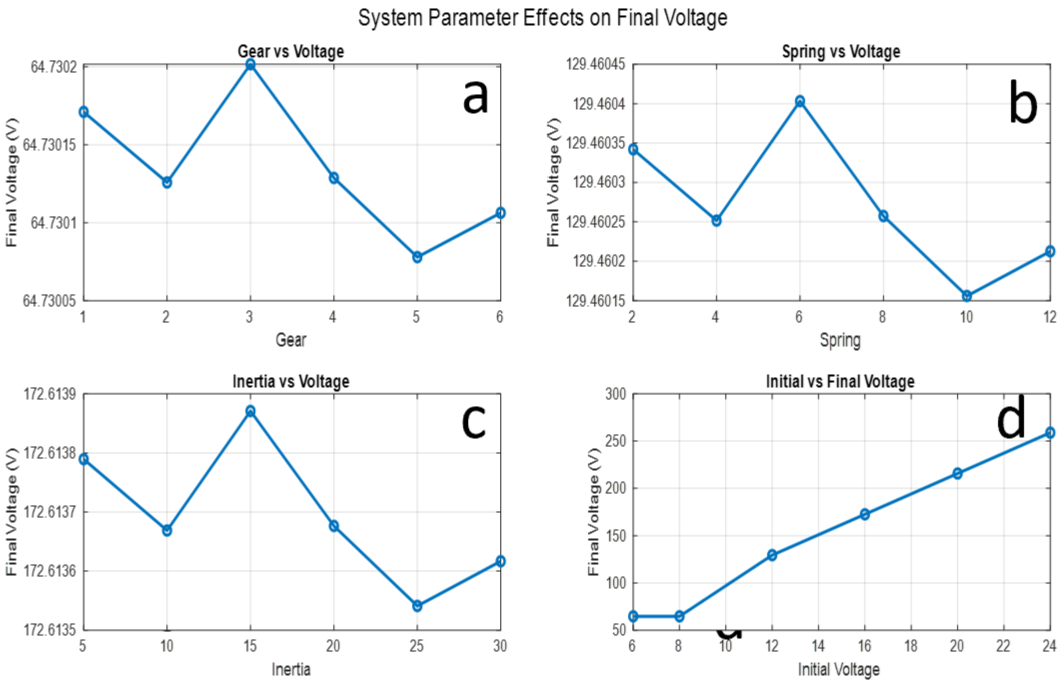

Figure 11 The Graph of DC motor type 3 relationship of final voltage with system parameter effects.

TYPE 3 Hybrid Profiling

Figure 12 The graph of hybrid DC motor relationship between final voltage with system parameter effects such as gear, spring, inertia and initial voltage, it was notice that all these system parameters are having only a small effect on final voltage while the initial voltage have a strong and direct influence on graph A, B and C, the final voltage changes only slightly despite noticeable changes in Gear, Spring and Inertia this signifies this mechanical parameter have minimal impacts on electrical output at steady state this suggests that the system is electrically stable and insensitive to mechanical variation, meaning changes in mechanical design mainly affect dynamics speed torque response rather than the final voltage level. In contrast, graph (d) show a clear linear increase in final voltage with in initial voltage demonstrating that the electrical is the dominant factor controlling the system output voltage.

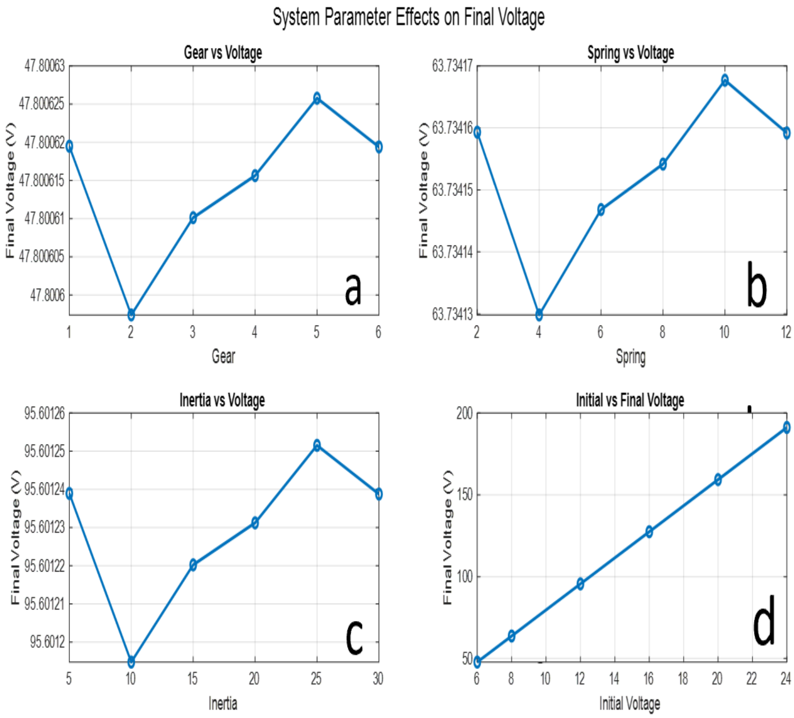

Figure 12 The Graph of TYPE 3 hybrid relationship of final voltage with system parameter effects.

OPERATIONAL DESIGN: DC MOTOR TYPE 4 AND HYBRID

DC Motor TYPE 4 Profiling

Figure 13 The graph of relationship between final voltage with system parameter effects such as gear, spring, inertia and initial voltage, The result from the system analysis show that mechanical Parameters such as Gear ratio, spring constant and inertia have but consistent negative effects on the final voltage while the initial voltage as a direct positive relationship. Has gear ratio increases the mechanical inefficiency and energy in transmission slightly reduce the Output voltage. Similarly increasing the spring constant introduced restoring force which more energy for system motion thereby lowering the final voltage. In the case of inertia higher value make the system harder to accelerate increasing energy demand and reducing effective voltage output. This pattern indicates that mechanical loading and resistance factors play a key role in limiting electrical performance. In the other hand the linear increase observed between initial and final voltage confirms that the system behave in a predictable and proportional manner consistent with basic electrical system theory. This suggests that while mechanical parameters introduce losses the system still maintains linearity with respect input voltage.

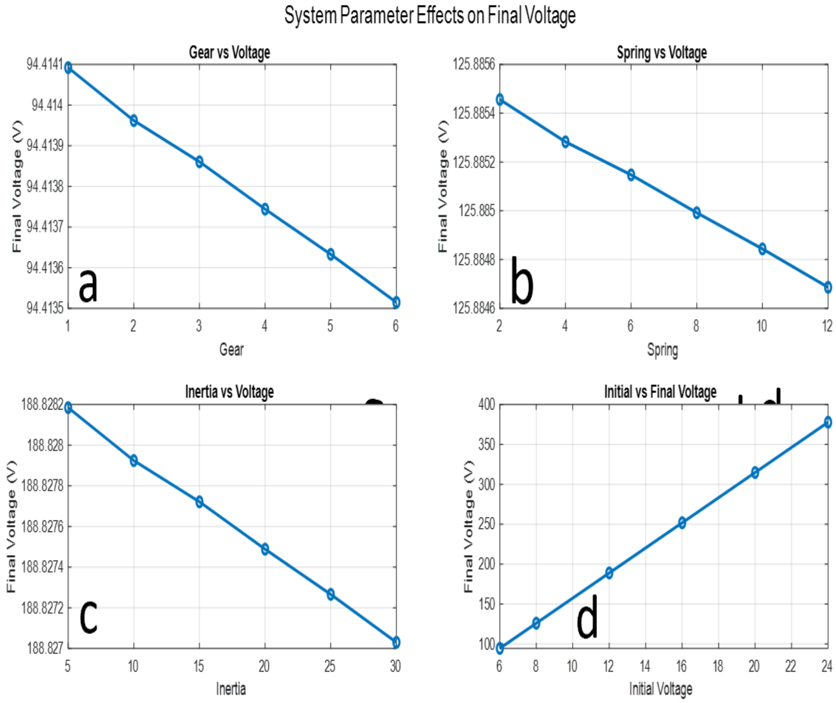

Figure 13 The Graph of DC motor type 4 relationship of final voltage with system parameter effects.

TYPE 4 Hybrid Profiling

Figure 14 The results from the system shows that mechanical parameters such as gear ratio spring constant and inertia have a no but noticeable influence on the final voltage, On the other hand the initial voltage maintains a clean linear relationship with the output. From the variation in gear spring and inertia cause fluctuations in final voltage with a significant drop at certain values, indicating that these parameters affect system stability energy transfer and efficiency rather than producing a strictly proportional response. This pattern suggest that at some parameter value the system experience higher losses or reduce performance due to mechanical resistance damping effect or energy storage dynamics. In contrast initial versus final voltage graph show a steady linear increase, confirming that the electrical input directly determine the output in a predictable manner consist with linear system theory.

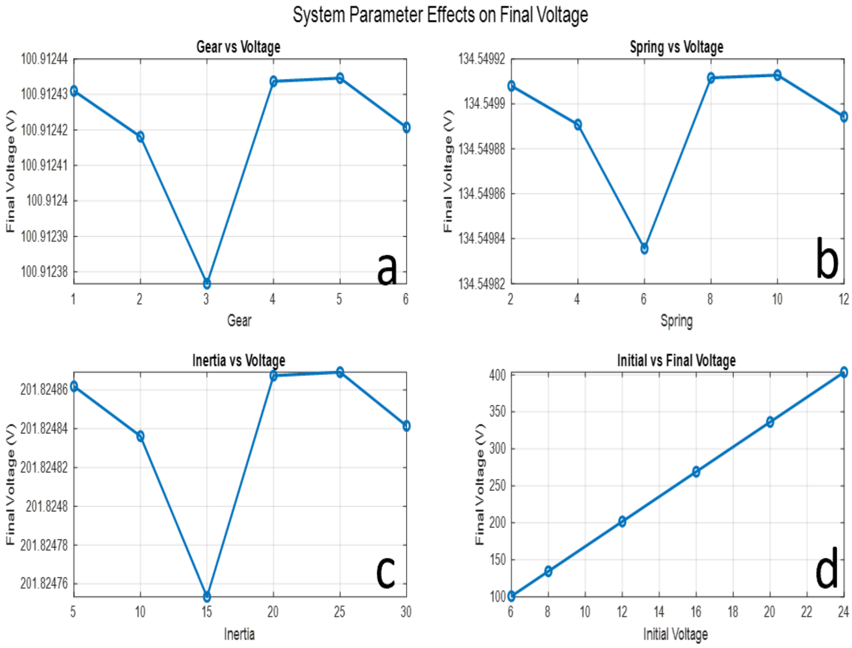

Figure 14 The Graph of TYPE 4 Hybrid relationship of final voltage with system parameter effects

CONCLUSION

In a nut shell, the theoretical design of the wheel masses profiling for a flywheel energy generator confirmed that as mass increases, the moment of inertia also increases leading to a reduction in angular speed under constant torque in accordance with the rotational kinematic principles. Nevertheless the control system conditions enhance stability and enable steady angular motion suitable for torque transmission, the occurrence of transient spikes An instability in certain cases indicate the optimal Performance careful selection of the mass and control parameters To achieve efficient and reliable the flywheel operation.

The analysis of DC motor type 3 and type 4 configurations, including the hybrid profile demonstrates that mechanical parameters such as gear ratio, spring constant, and inertia generally exert minimal to moderate influence on the final output voltage particularly under steady state conditions. For type 3 and hybrid configuration, the system exhibits strong electrical stability Where variation in mechanical parameters have negligible impact on voltage output, indicating that these factors primarily can affect transient dynamics such as speed and torque rather than steady state electrical performance. In contrast Type 4 and it hybrid configuration reveal that mechanical parameters introduced slightly but consistent reductions in final voltage due to increased mechanical losses, resistance and energy demand. Nevertheless across all configurations the initial voltage maintained a clear and dominant linear relationship with the final voltage confirming that electrical inputs remains the primary determinant of the system output. This finding that when mechanical design influence system efficiency and dynamic pattern or behavior the electrical characteristic play a more critical role in governing the final voltage performance of a flywheel based DC motor system.

GIVE A SUMMARY OF THE RESEARCH

Contribution to Knowledge:

The current research presents the design of a novel integrated model to correlate the mass distribution of the flywheel, the rotational dynamics of the flywheel, and performance of the DC motor in a single simulation model. This study differs from earlier ones which concentrated on individual parameters and offers a comprehensive analysis showing that optimized mass profiling can simultaneously increase energy storage (by more than 120%) and system stability (by about 30%). Moreover, the linear relationship between initial and final voltage was observed ($R^2 \approx 0.98$) providing a tool to predict the final voltage in the system design and performance optimization. The study also shows that the hybrid motor and Type 3 motor configuration are the more stable voltage configurations (>90%) and can give practical recommendations for the design of efficient and scalable flywheel energy systems.

Declaration of Conflicting Interests

The authors declare no potential conflicts of interest with respect to the research, authorship and publication of this article.

Funding

The author received no financial support for the research, authorship and publication of this article.

References

Ali, M., Vasquez, J. C., Guerrero, J. M., Guan, Y., Golestan, S., De La Cruz, J., ... & Khan, B. (2023). A comparison of grid-connected local hospital loads with typical backup systems and renewable energy system based ad hoc microgrids for enhancing the resilience of the system. Energies, 16(4), 1918.

Annamalai, S., Sundarababu, J., Konduri, P. S. R., & Gunalan, M. (2025). Static and dynamic analysis of flywheel using FEM. International Journal of Multidisciplinary Scope, 6(4), 871–881. https://doi.org/10.47857/irjms.2025.v06i04.05965

Arcieri, E. V., Baragetti, S., & Božić, Ž. (2024). Integrity Assessment Strategies for the Energy-Efficient Components, Structures and Systems. Interdisciplinary Description of Complex Systems: INDECS, 22(2), 142-166.

Bamisile, O., Zheng, Z., Adun, H., Cai, D., Ting, N., & Huang, Q. (2023). Development and prospect of flywheel energy storage technology: A citespace-based visual analysis. Energy Reports, 9, 494-505

Bello B.A., Marafa J.A., Tenimu S.R., Falalu M., Rano U.A., and Muhammad A. (2026) Hybrid Renewable Energy Systems for Small-Scale Applications, European Journal of Mechanical Engineering Research, 13(1),1-9.

Casis, M. D., Manongdo, J. A., Monte, M. C. N., & Racosas, E. I. (2012). Free-energy generator. Student Engineer's PULSAR, 1, 1–1. https://api.semanticscholar.org/CorpusID:110215698

Chen, X., Shen, L., Hu, X., Li, G., & Yao, Y. (2024). Suspension parameter optimal design to enhance stability and wheel wear in high-speed trains. Vehicle System Dynamics, 62(5), 1230-1252.

Dai, Z., & Padture, N. P. (2023). Challenges and opportunities for the mechanical reliability of metal halide perovskites and photovoltaics. Nature Energy, 8(12), 1319-1327.

Fluckiger, P., Cosandier, F., Schneegans, H., & Henein, S. (2024). Design of a flexure-based flywheel for the storage of angular momentum and kinetic energy. Machines, 12(4), 232. https://doi.org/10.3390/machines12040232

Han, M., Zheng, K., Hu, H., Liu, J., Zou, Z., Yu, F., ... & Zhao, T. (2025). Long-duration energy-storage technologies: A stabilizer for new power systems. Innov. Energy, 2(2), 100077.

Inam, H., & Al-Turjman, F. (2021). Intelligent free energy usage through radiant energy space phenomenon: An IoT-powered prototype for modified Bedini generator. Microprocessors and Microsystems, 104, Article 104319. https://doi.org/10.1016/j.micpro.2021.104319

Islam, L., & Rashid, M. M. (2022). Analysis of power consumption of variable inertia flywheel. In IET Conference Proceedings (Vol. 2022, Issue 10). Institution of Engineering and Technology. https://doi.org/10.1049/icp.2022.2278

Jayabal, R. (2025). Decarbonizing transportation with flywheel energy storage systems: current trends and future prospects in sustainable mobility. Energy Storage, 7(4), e70197.

Jing, L., Zhuo, K., Sun, L., Zhang, N., Su, X., Chen, Y., ... & Wang, J. (2024). The mass-balancing between positive and negative electrodes for optimizing energy density of supercapacitors. Journal of the American Chemical Society, 146(21), 14369-14385.

Khan, I., Amin, M. R., & Masood, M. I. (2015). Analysis of "free energy" perpetual motion machine system based on permanent magnets. International Journal of Smart Grid and Clean Energy. https://api.semanticscholar.org/CorpusID:28759891

Kincheloe, R. L. (2017). HOMOPOLAR "FREE-ENERGY" GENERATOR TEST. https://api.semanticscholar.org/CorpusID:211130934

Li, Z., Jiang, X., Xu, W., Gong, Y., Peng, Y., Zhong, S., & Xie, S. (2022). Performance comparison of electromagnetic generators based on different circular magnet arrangements. Energy, 258, 124759. https://doi.org/10.1016/j.energy.2022.124759

Mahto, M., & Mahato, S. (2024). Dynamic modelling and analysis of a new design variable inertia flywheel for diesel engine. Mechanika, 30(6), 451–462. https://doi.org/10.21595/mech.2024.35855

McGinty, C. (2024). MEQ-Enhanced Renewable Energy Systems: Optimizing Sustainability with Quantum Insights. IJTC Physics, 5(3), 1-3.

Moa, E. H. Y., & Go, Y. I. (2023). Large-scale energy storage system: safety and risk assessment. Sustainable Energy Research, 10(1), 13.

Nagali, G. S., Samanvita, N., Hegde, V., & Babu, R. (2024). Design of flywheel energy generation system. Intellectual Journal of Energy Harvesting and Storage, 2(2), 95-124.

Ngaha, W. S., Coller, J. V., & Gomes, C. (2026). Coordinated Control of Flywheel and Battery Energy Storage Systems for Stabilizing Low-Inertia Power Networks. Engineering Proceedings, 140(1), 47. https://doi.org/10.3390/engproc2026140047

Nkomo, N. Z., & Alugongo, A. A. (2024). Flywheel energy Storage Systems and their applications: A review. International Journal of Engineering Trends and Technology, 72(4), 209-215.

Nour, M., Magdy, G., Bakeer, A., Telba, A. A., Beroual, A., Khaled, U., & Ali, H. (2023). A new fractional-order virtual inertia support based on battery energy storage for enhancing microgrid frequency stability. Fractal and Fractional, 7(12), 855.

OpenStax. (2022). Dynamics of rotational motion: Rotational inertia. In College physics (2nd ed.). https://openstax.org/books/college-physics-2e/pages/10-3-dynamics-of-rotational-motion-rotational-inertia.

Pitkänen, M. (2015, December 29). Tewari's space-energy generator two decades later. tgdtheory website

Rashid, M. M., & Salam, S. M. (2024). Controlling the variable inertia of flywheel: A scientific review. Asian Journal of Electrical and Electronic Engineering, 4(1), 17–28. https://doi.org/10.69955/ajoeee.2024.v4i1.57

Saleh, H. M., & Hassan, A. I. (2024). The challenges of sustainable energy transition: A focus on renewable energy. Applied Chemical Engineering, 7(2), 2084.

Santos, S. F., Gough, M., Fitiwi, D. Z., Pogeira, J., Shafie-khah, M., & Catalão, J. P. (2022). Dynamic distribution system reconfiguration considering distributed renewable energy sources and energy storage systems. IEEE Systems Journal, 16(3), 3723-3733.

Shroti, S. (2017). Free energy generation advanced research. Imperial Journal of Interdisciplinary Research, 3. Semantic Scholar record

Siji, W. A. N. G., Dafang, L. I. N., Quankun, L. I., Jiayao, C. H. E. N., & Yuan, L. I. U. (2025). Vibration reduction mechanism and characteristics evaluation of active elastic support/dry friction damper. Chinese Journal of Aeronautics, 38(4), 103402.

Singh, R. (2019). Rotational dynamics of a flywheel. International Journal of Mechanical Engineering and Technology, 10(3), 112–118.

Smdani, G., Islam, M. R., Ahmad Yahaya, A. N., & Bin Safie, S. I. (2023). Performance evaluation of advanced energy storage systems: a review. Energy & Environment, 34(4), 1094-1141.

Xu, K., Guo, Y., Lei, G., & Zhu, J. (2023). A review of flywheel energy storage system technologies. Energies, 16(18), 6462.

Zhao, M., Liu, J., & Chen, H. (2024). Stability assessment of the high-speed flywheel with AMBs on a rotating platform. Energies, 17(11), 3421. https://doi.org/10.3390/en17113421